

# The physics and modes of star cluster formation: simulations

BY CATHIE CLARKE

*Institute of Astronomy, University of Cambridge, Madingley Road, Cambridge  
CB3 0HA, UK*

We review progress in numerical simulations of star cluster formation. These simulations involve the bottom-up assembly of clusters through hierarchical mergers, which produces a fractal stellar distribution at young ( $\sim 0.5$  Myr) ages. The resulting clusters are predicted to be mildly aspherical and highly mass-segregated, except in the immediate aftermath of mergers. The upper initial mass function within individual clusters is generally somewhat flatter than for the aggregate population. Recent work has begun to clarify the factors that control the mean stellar mass in a star-forming cloud and also the efficiency of star formation. The former is sensitive to the thermal properties of the gas while the latter depends both on the magnetic field and the initial degree of gravitational boundedness of the natal cloud. Unmagnetized clouds that are initially bound undergo rapid collapse, which is difficult to reverse by ionization feedback or stellar winds.

**Keywords:** hydrodynamics; stars: formation; stars: mass function; open clusters and associations: general

## 1. Introduction

Hydrodynamic simulations of star cluster formation are in their infancy. This is hardly surprising, since only in the last decade has it been possible to move beyond modelling the formation of single stars and binaries. Even with current high-performance-computing facilities, it is still unfeasible to undertake cluster simulations that can follow the collapse of individual stars down to stellar densities (cf. Bate 1998). Thus, ‘star formation’ in the simulations actually means the accumulation of gravitationally bound gas within ‘sink particles’ of specified radius. In general, the most ambitious simulations (in terms of numbers of stars formed and, hence, the ability to track hierarchical cluster assembly) are those that necessarily use rather large sink radii. This suppresses the proper modelling of close-binary formation (see Goodwin 2010) and compromises the modelling of stellar dynamical interactions. Other shortcomings include the fact that most simulations to date omit magnetic fields and model the gas using a simple barotropic equation of state.

These shortcomings should not detract from the achievement of being able to model the hydrodynamics of cluster formation at all. First, it should be stressed that there are a number of ongoing efforts to add new physical ingredients to the simulations, including magnetic fields, radiative transfer and the effects of thermal and mechanical feedback. Second, however, it should be borne in mind that even in their simplest, ‘vanilla’ forms, these simulations represent an enormous advance on

attempts to model young clusters as an  $N$ -body system plus background potential (e.g., Geyer & Burkert 2001; Boily & Kroupa 2003).

Although such simulations can be valuable in studying the later stages of cluster dispersal, once star formation has ceased (Goodwin & Bastian 2006), they are no substitute during the early, embedded phase of cluster evolution for hydrodynamical simulations that can capture the complex interplay between fragmentation, accretion, infall and stellar dynamics. This review concentrates on predictions of those ‘turbulent-fragmentation’ simulations that have been most thoroughly analysed to date. The discussion will, therefore, focus on observables (e.g., mass segregation, mass functions, clustering statistics, cluster morphology) and should therefore be read in conjunction with Lada (2010), who reports on the current observational status in these areas. This is followed by a preliminary survey of the results to date from simulations that include a more complete suite of input physics. Finally, we try and link the insights gained from such simulations to issues of star formation on a Galactic scale.

Before embarking on this description, it is worth stressing that the simulations described here relate to the very earliest (deeply embedded) phases of cluster formation, typically covering about the first 0.5 Myr following collapse of the parent cloud. Clustering statistics are still evolving at the end of these simulations. Consequently, questions of ultimate cluster survival have to be followed over considerably longer timescales [see the discussion of cluster ‘infant mortality’ by de Grijs (2010)].

## 2. An overview of cluster-formation simulations

### (a) *Setting up of ‘turbulence’ in the cluster-formation context*

It is now well-established that molecular clouds evidence supersonic internal motions whose energy is similar to the gravitational potential energy of the cloud (Larson 1981; Heyer *et al.* 2001; Heyer & Brunt 2004). Thus, molecular cloud complexes are likely to contain both regions that are somewhat bound and somewhat unbound and this is an important factor in determining the star-formation efficiency and merger history of clusters locally (Clark & Bonnell 2004; Clark *et al.* 2008). The observed ‘size–linewidth’ relation in molecular clouds (Larson 1981) implies a velocity power spectrum with index  $P(k) \propto k^{-4}$ . This similarity to the spectra of Kolmogorov or Burgers turbulence has encouraged an interpretation in terms of a cascade of energy from some large scale where it is being continuously injected. Grid-based simulations (e.g., Kritsuk *et al.* 2007; Lemaster & Stone 2008; Kitsionas *et al.* 2008) are well suited to modelling the resulting turbulent density fields.

Such simulations, however, do not include self-gravity and so the stellar mass functions derived from such simulations are obtained a posteriori by identifying what would be Jeans-unstable fragments in the density field (Padoan *et al.* 1997). Naturally, such (zero-gravity) calculations cannot follow cluster formation and evolution. We therefore concentrate here on self-gravitating calculations, which (for the large-scale calculations discussed here) means Lagrangian (smoothed-particle hydrodynamics; henceforth SPH) calculations [see Chapman *et al.* (1992) and Klessen *et al.* (1998) for the earliest examples of cluster-formation simulations]. These treat the velocity field in two ways. Those of Klessen and collaborators (e.g., Schmeja & Klessen 2004) impose continuous forcing of the velocity field at some range of

input scales, so that (as in the calculations of Padoan and collaborators) a quasi-stationary turbulent cascade is set up.

Bonnell, Bate and co-workers instead introduce internal motions in the cloud as a one-off initial input. Dissipation of these motions means that star formation and cluster merging proceeds over one or two global free-fall timescales, since there is no continuous injection of kinetic energy to support the cloud. In this case, the velocity field of the gas over a free-fall time is just inherited from the initial conditions and therefore for the velocity field to match the observed size–linewidth relation, they require a particular input velocity power spectrum, i.e.,  $P(k) \propto k^{-4}$ . It can justifiably be argued that such a situation is not one of true turbulence, as it does not reflect an equilibrium cascade of energy from large to small scales. Nevertheless, we will use the term ‘turbulent’ in the loose way that has become common currency in the field. The reader should bear in mind that this merely denotes a situation where the gas is (either initially or continuously) subject to supersonic internal motions.

(b) *Structure formation and the implementation of star formation*

Supersonic turbulent motions lead to the formation of shocked layers which, under the action of self-gravity, fragment into filaments and then into bound objects. The computational expense of following the hydrodynamic collapse of extremely dense gas is avoided through the implementation of ‘sink particles’ (Bate *et al.* 1995), which interact gravitationally with the rest of the calculation and can also continue to accrete bound gas that enters within the sink radius. The exact criterion for sink-particle creation changes slightly between calculations, but usually involves the requirement that  $\sim 100$  bound SPH particles are contained within the sink at some minimum threshold density (whose value varies between different simulations in the range  $\sim 10^{-13} - 10^{-11} \text{ g cm}^{-3}$ ). We will henceforth describe sink particles as ‘stars’; however, in the largest-scale simulations, the sink radius is as large as 50 AU (Bonnell *et al.* 2003, 2004), so that modelling of both discs and close-binary companions is thus impossible in these simulations.

(c) *Evolution following the onset of star formation*

Stars typically form first in the dense gas at the intersection of collapsing filaments (see figure 1). Gas and stars forming along the filaments’ lengths fall in towards the local potential minimum and a protocluster is then established (e.g., Klessen & Burkert 2000, 2001; Bate *et al.* 2003; Bonnell *et al.* 2003). This is a small-scale system initially and, therefore, few-body interactions are particularly important for the first stars to form, especially in simulations with small sink radii (Bate *et al.* 2003) which can model interactions with moderately hard binaries (separations of a few AU). The infalling gas possesses angular momentum because of the vorticity of the initial velocity field, and where the cluster centre is dominated by a single massive star, it frequently acquires a large-scale disc (see lower panels in figure 1). This then fragments copiously, adding new stars to the cluster in addition to those that arrive entrained in the infalling gas. [Note that this very copious fragmentation of circumstellar discs is an artefact of the equation of state used in most such calculations: see Bate (2009b) and §4a.] The initial mass of sink

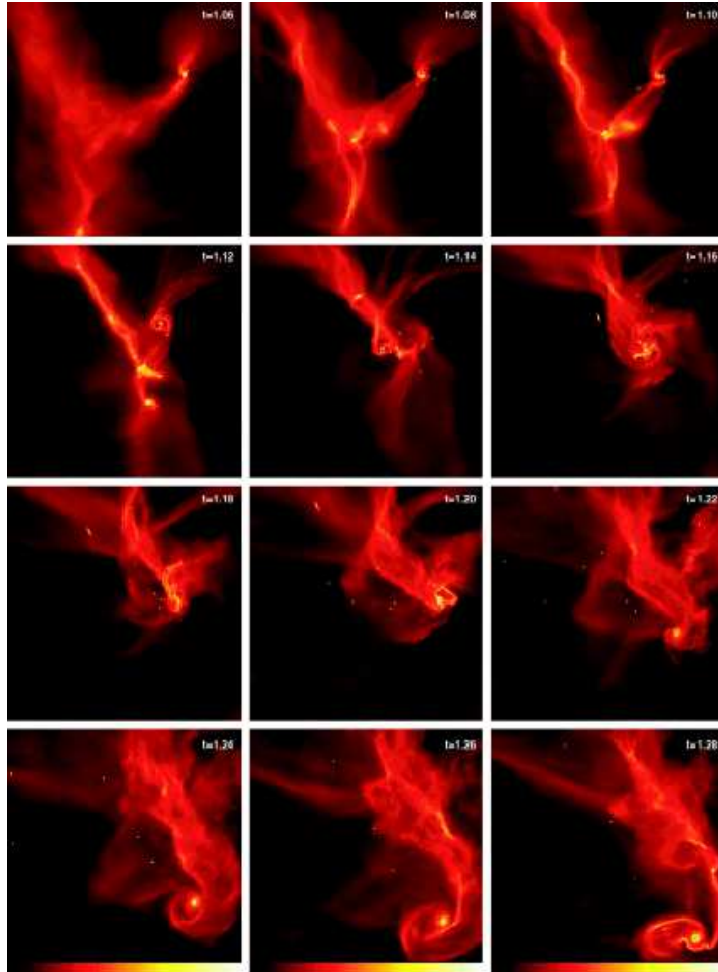


Figure 1. Evolutionary sequence for cluster formation (Bate *et al.* 2003).

particles is very small ( $\sim 10^{-3} M_{\odot}$ ). They rapidly accrete the core of bound gas in their vicinity but then, depending on their local environment, may also continue to accrete significantly over much longer periods. This is particularly true of the most massive stars, which rapidly segregate to the gas-rich protocluster core.

This differential acquisition of mass according to a star’s current mass is known as ‘competitive accretion’ and was originally understood in an idealized way in terms of Bondi–Hoyle accretion, whereby the accretion cross section of a star scales quadratically with its mass (Bondi & Hoyle 1944). This accretion law causes a narrow range of initial masses to be mapped onto a power-law distribution of final masses, in which the fraction of stars with mass  $M$  in a given linear mass interval scales as  $M^{-2}$  (Zinnecker 1982), suggestively close to the Salpeter slope of  $M^{-2.35}$  (Salpeter 1955). Subsequently, Bonnell *et al.* (2001) analysed competitive accretion in the context of ‘plum pudding’ models, in which stellar-mass points are embedded in a smooth collapsing gas sphere. In the outer cluster, the stars almost co-move

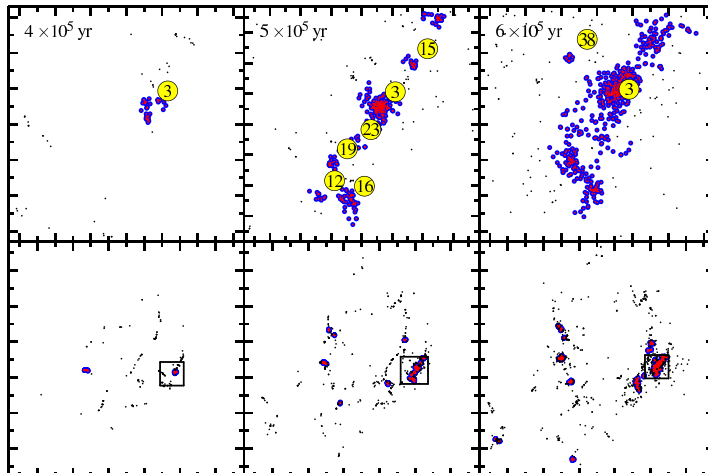


Figure 2. Evolution of clustering in the simulation of Bonnell *et al.* (2008). The upper panel (scale  $0.6 \times 0.6 \text{ pc}^2$ ) is an enlargement of the boxed region in the lower panel (scale  $6 \times 6 \text{ pc}^2$ ). (From Maschberger *et al.* 2009).

with the gas and, hence, the relevant cross section is set by the star’s tidal radius rather than its (much larger) Bondi–Hoyle radius. In this limit, the resulting IMF is predicted to be flatter ( $\propto M^{-1.5}$ ) and Bonnell *et al.* ascribed the IMF in the simulations (flatter at low mass and steepening to a Salpeter-like high-mass tail) to competitive accretion in the tidally limited and Bondi–Hoyle regimes, respectively. It is remarkable, given the much more complex dynamical histories of stars in the turbulent-fragmentation calculations compared with the simple radial infall in plum pudding models, combined with the extremely inhomogeneous density fields in the turbulent case, that turbulent-fragmentation calculations also produce an IMF of this form (e.g., Bate *et al.* 2003; Bonnell *et al.* 2006; see figure 4).

Another aspect of competitive accretion is that the original provenance of accreted material depends on a star’s mass. A low-mass star, which remains of low mass (perhaps due to a dynamical interaction that ejects it from its natal proto-cluster) just accretes the overdense gas surrounding the sink particle at the time of its creation. Stars that end up with high masses have protracted accretion histories. They acquire mass from a variety of locations in the initial cloud (Bonnell *et al.* 2004).

(d) *The evolution of clustering: a bottom-up process*

Clustering in the simulations is a natural outcome of the highly inhomogeneous density fields in turbulent clouds which are amplified by gravitational collapse. It is a bottom-up process: the basic unit of cluster formation is a small- $N$  group which successively merges with larger entities. This requires a qualitative shift in our view of cluster formation, away from traditional (monolithic-collapse) models.

Figure 2 depicts the evolution of the stellar density distributions in the simulation of Bonnell *et al.* (2008), while figure 3 represents the corresponding merger tree (Maschberger *et al.* 2009). Clusters are extracted from the projected stellar

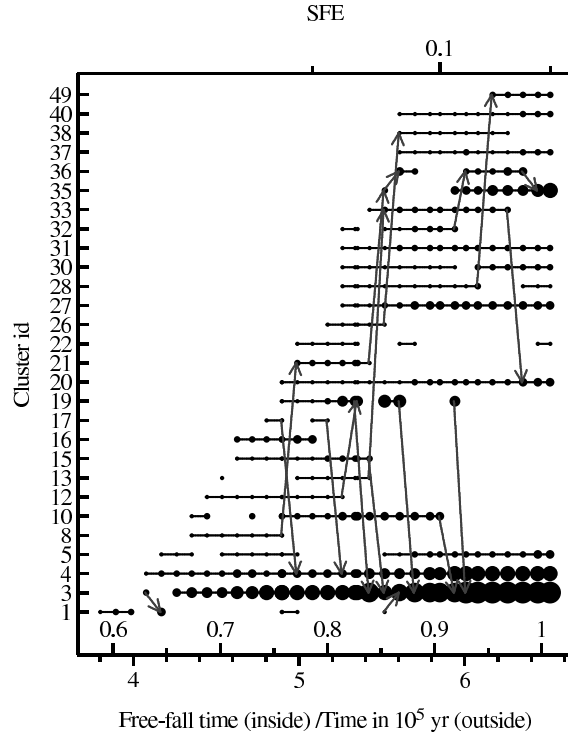


Figure 3. Cluster merger tree from Maschberger *et al.* (2009) for the simulation shown in figure 2. The symbol size denotes the richness of the cluster.

distributions using a minimum spanning tree (Cartwright & Whitworth 2004). The lower panel of figure 2 illustrates the global evolution, wherein the left-hand part of the simulation (which was initially mildly unbound) forms a number of relatively isolated clusters and a pronounced field population (small dots), while the boxed region (on which the upper panel zooms in) undergoes a runaway merger to a single cluster.

### 3. Observational predictions of ‘vanilla’ calculations

We now examine the detailed results of what can be termed ‘vanilla’ calculations, i.e., those including the minimal subset of physical effects that are required for turbulent fragmentation to occur. Such calculations are Lagrangian (SPH) and involve imposition of supersonic internal motions. These simplest calculations omit magnetic fields and apply a barotropic equation of state, which is a parameterization of the results of spherically symmetric collapse calculations modelled with frequency-dependent radiative transfer (Masanuga & Inutsuka 2000). Here, we focus on large-scale calculations that model the formation of at least hundreds of stars, so that we can analyse the history of cluster assembly and the relationship to the IMF. Readers with an interest in detailed predictions of the multiplicity characteristics of smaller-scale cores are referred to Delgado–Donate *et al.* (2003, 2004*a,b*), Goodwin *et al.* (2004*a,b*, 2006) and Offner *et al.* (2009).

The calculations we discuss here are (i) those of Klessen and collaborators (e.g., Klessen 2001; Schmeja & Klessen 2004), which employ periodic-box boundary conditions and a continual forcing of the velocity field over a prescribed range of spatial scales. Both effects counteract the global collapse that is seen in the other simulations, although there is local collapse of regions where the ratio of gravitational to kinetic energy is large; (ii) those of Bate *et al.* (Bate *et al.* 2003; Bate 2009c) which focus on relatively small-scale systems ( $\sim 50 M_{\odot}$ ) to attain a good mass resolution and small sink radius (note that Bate 2009a most recently extended such high-resolution studies to larger clouds of  $500 M_{\odot}$ ). These calculations are particularly well suited to the study of the low-mass end of the IMF and best capture the formation and dynamical interactions of close binaries; (iii) larger-scale simulations which sacrifice mass and spatial resolution to be able to model a statistically large ensemble of stars. These calculations are thus optimal for studying the upper end of the IMF and the hierarchical merging of clusters.

Much of what follows is based on the analysis of Maschberger *et al.* (2009) of a  $10^3 M_{\odot}$  simulation (reported in Bonnell *et al.* 2003, 2004) and a similar  $10^4 M_{\odot}$  simulation (reported in Bonnell *et al.* 2008). However, we caution that it may be impossible to sacrifice resolution on small scales without affecting the behaviour of the simulation on larger scales. The large sink radius in these calculations (50 AU) suppresses the role of dynamical interactions with even moderately hard binaries (with separations of tens of AU) and therefore dynamical ejections play a less important role in these simulations than in higher-resolution calculations. Higher-resolution ‘vanilla’ calculations are, however, not necessarily more realistic since, in contrast to the larger-scale simulations, they probably *over*predict the role of close dynamical interactions because they overproduce close companions (see §4a).

#### (a) *The formation of brown dwarfs*

The low-mass end of the IMF is populated by objects that form in high-density gas (where the Jeans mass is relatively small) and whose subsequent dynamical history does not cause them to continue to accrete at a high rate. In practice, the high-density regions of the simulation are either dense filaments or circumstellar discs (Bate *et al.* 2002). As noted above, the profuse fragmentation of circumstellar discs in the simulations of Bate *et al.* (2002, 2003, 2009a) overproduces brown dwarfs, yielding a brown-dwarf-to-star number ratio of at least 3 : 2 compared with the observed estimate of 1 : 3 (Andersen *et al.* 2008). This shortcoming in the barotropic calculations has, however, been largely remedied by the inclusion of magnetic fields and radiative feedback (see §a).

The requirement of low accretion rates (such that brown dwarfs remain brown dwarfs) is achieved in two ways in the simulations. In the high-resolution simulations, the principal mechanism is through dynamical ejections from regions of dense gas (Reipurth & Clarke 2001). In low-resolution simulations, which suppress such effects, another mechanism becomes apparent whereby brown dwarfs form in dense, infalling filaments: here it is the tidal shear of such filaments as they fall into the cluster potential that draws gas away from collapsing condensations and thus ensures a low final mass (Bonnell *et al.* 2008).

It should be stressed that, in contrast to the early speculations of Reipurth & Clarke (2001), the process of dynamical ejection does not impart the resulting

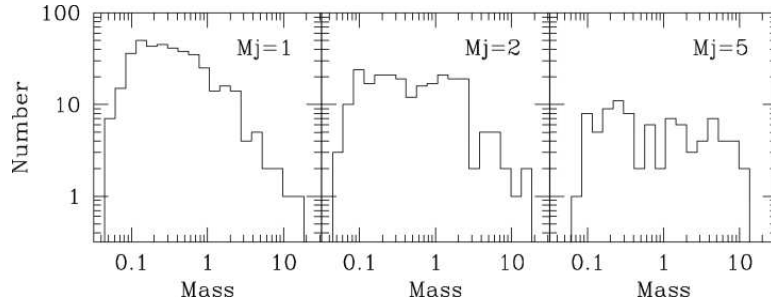


Figure 4. The IMF produced in isothermal simulations of Bonnell *et al.* (2006) for three different values of the initial Jeans mass ( $M_J$ , in units of  $M_\odot$ ). Note that the ‘knee’ of the IMF simply tracks  $M_J$ .

brown-dwarf population with a higher velocity dispersion than the higher-mass stars. A clear observational hallmark of the importance of dynamical interactions is that binary stars in the simulations on average have a lower velocity dispersion than single stars (Bate *et al.* 2009*a*; see also Delgado-Donate *et al.* 2003).

(b) *The ‘knee’ of the IMF*

The IMF shown in figure 4 has the property that its power-law slope (such that the fraction of stars in the mass range  $M$  to  $M + dM$  scales as  $M^{-\alpha}$ ) makes a transition from  $\alpha < 2$  to  $\alpha > 2$  at a mass scale of  $\sim 1 M_\odot$ . Since the mean stellar mass of a power-law distribution is dominated by the upper (lower) mass limits for  $\alpha < (>)2$ , we see that such a rollover imparts the IMF with a characteristic stellar mass at around this mass scale. The observed IMF (Kroupa *et al.* 1993) shows similar behaviour and raises the issue of the origin of this mass scale.

In the first generation of simulations (Bate & Bonnell 2005), the characteristic mass scaled simply with the average Jeans mass in the *initial cloud*. Padoan *et al.* (1997) (see also Clarke & Bromm 2003) had previously argued that the mass scale is instead set by the Jeans mass in the *shocked gas* and would therefore depend on the Mach number of the turbulence. Although the Mach number undoubtedly influences the density distribution attained in the simulations, the full hydrodynamical calculations demonstrate that it has little effect on the resulting IMF, probably because it is inappropriate to apply the spherical Jeans criterion to shocked layers (Elmegreen & Elmegreen 1978; Lubow & Pringle 1993; Clarke 1999).

There is, however, a glaring problem with any theory which links the characteristic mass scale of the IMF with the gross properties of the parent cloud, i.e., in which the characteristic stellar mass varies as  $T^{1.5}/\bar{\rho}^{1/2}$ . The order-of-magnitude variations in the temperature ( $T$ ) of molecular clouds, together with the difficulty of defining a mean density ( $\bar{\rho}$ ) in a fractally organized interstellar medium (ISM), means that one would expect considerable variation in the IMF knee in different star-forming regions. Instead, this is found to be surprisingly invariant in all well-studied regions (Kroupa 2002; Muench *et al.* 2002; Chabrier 2003). Clearly, therefore, we need a theory which breaks the dependence of characteristic mass scale on gross cloud properties and which instead invokes a physical process to set a characteristic density and temperature.



To date, there are two (distinct) modifications of the simplest barotropic equation of state used in the early calculations that can break the mapping between mean cloud properties and characteristic stellar mass scale. Bonnell *et al.* (2006) replaced the strictly isothermal equation of state (at densities below  $10^{-13}$  g cm $^{-3}$ ) by one which switched between mild cooling to mild heating at a density of  $3 \times 10^{-18}$  g cm $^{-3}$ . This prescription is motivated by the arguments contained in Larson (2005), who identifies the change in barotropic index with the onset of efficient dust–gas coupling at this density (see also Whitworth *et al.* 1998). With this equation of state, Bonnell *et al.* were then able to produce indistinguishable IMFs in simulations with quite different parent-cloud parameters.

We stress that these results refer to the *stellar* IMFs produced by the simulations: although there is considerable interest in the literature in relating this to the observed *core*-mass function (CMF; Motte *et al.* 1998; Lada *et al.* 2008; Myers 2008), the analysis of the simulations using a variety of CLUMPFIND-style algorithms (Smith *et al.* 2008) yields CMFs for which the ‘knee’ is a function of the details of the algorithm employed. Indeed, different observational studies do not always agree on the identity of individual clumps in a given region (Johnstone *et al.* 2000; Motte *et al.* 1998). Thus, although it is important for simulations to go beyond the reproduction of the stellar IMF and to also produce the correct structures in the ISM, it is difficult to establish, pending wider agreement on clump-extraction algorithms, whether or not this is the case.

Alternatively, the recent radiative-transfer simulations of Bate (2009*b*) also disconnect the IMF and the mean Jeans mass of the parent cloud. In this case, Bate argues that the characteristic mass scale is set not by a particular cooling regime, but by the fact that feedback from low-mass star formation produces a rather narrow spread in the Jeans mass of irradiated gas (see §4*a*).

### (c) *The high-mass tail of the IMF*

As noted above, the IMF in the simulations above the knee rolls over and approaches a power law in the high-mass regime. Obviously, this is much better sampled in the high-mass simulations. The simulations of Bonnell *et al.* (2003, 2008) are particularly suitable in this regard as at the end of the simulation they produce  $\sim 100$  and  $\sim 1000$  stars in the high-mass tail, respectively. The slope of this high-mass tail is  $\alpha = 2 \pm 0.2$ , with some mild evolution towards a flatter slope with time in regions where ongoing merging allows massive stars to continue to accrete vigorously.

A notable result is that the slope of the upper IMF is flatter (smaller  $\alpha$ ) within individual clusters than for the whole (cluster + field) population (figure 5). This is partly a consequence of mass segregation (see §3*e*), since the more massive stars are more likely located within clusters. We see indeed in figure 5 that the IMF for all stars in clusters is flatter than the IMF of the whole (cluster + field) population, since the stellar composition of the two samples is not identical.

This is, however, not the full story, since there is also a difference between the IMF within individual clusters and the IMF of the combined population of all stars in clusters. This implies that clusters are not simply randomly assembled from the total population of all stars in clusters. Kroupa & Weidner (2003) first pointed out that random drawing might not be a good cluster-assembly model and argued that

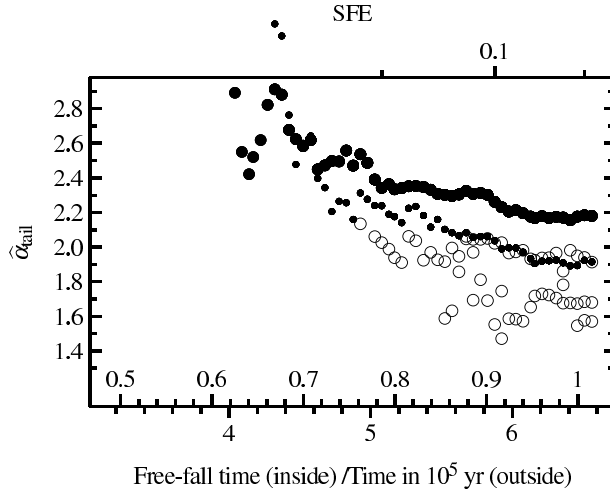


Figure 5. Exponent ( $\alpha$ ) of the upper IMF for individual clusters (open circles) for the whole simulation (large dots) and for all stars in clusters (small dots) as a function of time. (Based on the simulations of Bonnell *et al.* 2008; see Maschberger *et al.* 2009)

the integrated IMF for a galaxy (the IGIMF) might be steeper than the IMF in individual clusters. Weidner & Kroupa (2006) showed that this would result if the maximum mass of a star in a cluster is a *systematic* function of cluster mass. (We emphasize the term ‘systematic’, i.e. one needs a consistent suppression of massive-star formation in low-mass clusters, which is *stronger* than the merely statistical effect that, on average, the maximum mass in a randomly drawn sample is an increasing function of the sample size). In the simulations we see below that this effect indeed results from a (cluster-mass-dependent) truncation of the upper IMF in individual clusters.

(d) *The truncation of the upper IMF in cluster-formation simulations*

The upper IMF in the simulated clusters is best fit by *truncated power laws* for which the truncation mass depends on the cluster mass (Maschberger *et al.* 2009). We stress that these simulations do not include feedback, so there is no intrinsic mass scale at which accretion onto a star is halted. Instead, truncation results from the finite time that has elapsed since the formation of the oldest stars in the cluster, which limits the maximum stellar mass attained at a given time. Richer clusters create deeper gravitational potentials and, hence, a richer accretion environment, so the truncation mass is usually larger in richer clusters. We note that the oldest, most massive stars that end up in a particular cluster usually formed as a small- $N$  entity and that this group of stars travels together through successive mergers. Thus, the upper end of the IMF in the simulated clusters is characterized by a group of stars just below the truncation mass that are rather similar in mass. (We emphasize that the simulations extend only over  $\sim 0.5$  Myr and, hence, correspond to the deeply embedded phase of star formation: these age differences would be imperceptible once the stars emerged as optically visible sources).

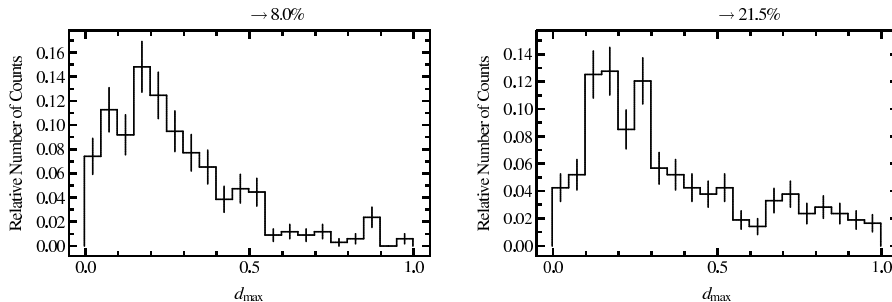


Figure 6. Histogram of fractional radial ranking of the most massive star in each cluster in the simulations of Bonnell *et al.* (2003; *left*) and Bonnell *et al.* (2008; *right*; see Maschberger *et al.* 2009).

(e) *Mass segregation in young clusters*

The simulations show pronounced mass segregation at an age of  $\sim 0.5$  Myr. This is demonstrated by figure 6, which shows the distribution of fractional radial rankings within their parent clusters of all stars that are the most massive members of their respective clusters. In the absence of mass segregation, this histogram would be flat, since the most massive stars would be equally likely to lie at any radial ranking. Instead, it is clearly peaked towards small values (the most massive star lies within its parent cluster’s half-number radius 80% of the time). Indeed, cases where the most massive star is significantly offset from its cluster’s centre correspond to situations of ongoing merging. Figure 6 demonstrates that periods when mass segregation would not be observed (cf. Bate 2009*a*) are relatively brief, implying that the mass-segregation timescale is generally shorter than the interval between successive mergers. Hence, mass segregation in clusters of this age should be the observational norm.

This mass segregation is ‘primordial’ in the sense that it is established when the cluster is very young by any observational standards. It is *not* primordial, however, in the sense that the most massive stars did not initially form within the cluster core (although they may have acquired much of their mass in this environment). Instead, the stars that end up with the highest mass are generally the first to form. Their headstart in mass acquisition means that they are likely to be deposited in the cluster core in each successive merger event. Mass segregation is thus a dynamical process, although the presence of gas and the highly nonequilibrium conditions mean that it is not well modelled as a purely two-body relaxation effect (see also Allison *et al.* 2009; de Grijs 2010).

(f) *Cluster morphology*

The projected ellipticities of clusters peak in the range 1 – 2 (figure 7). Clusters are thus mildly aspherical, which is a consequence of two competing tendencies: clusters form from condensations within filaments and cluster mergers often follow the filament morphology. Against this, however, stellar dynamical interactions in the merging cores tend to sphericalize the clusters. In general, the cluster cores are more dynamically relaxed (rounder) than their outer regions, which retain a greater memory of previous merger events.

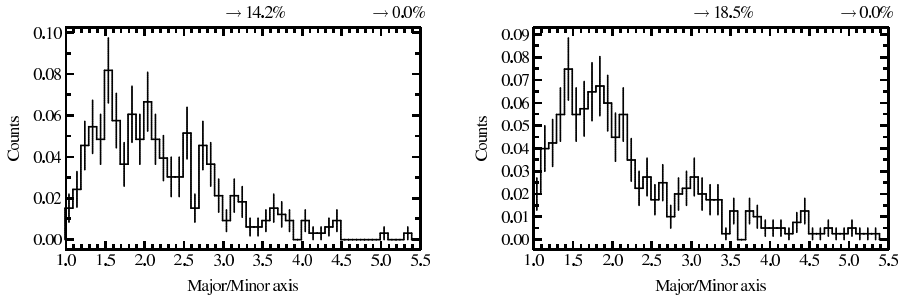


Figure 7. Distribution of projected cluster ellipticities in the simulations of Bonnell *et al.* (2003; *left*) and Bonnell *et al.* (2008; *right*; see Maschberger *et al.* 2009).

(g) *Dependence of stellar/cluster properties on initial conditions*

Several studies have experimented with changing the power spectrum of the ‘turbulent’ velocity field, the Mach number of the turbulence and the global gravitational boundedness (i.e., the ratio of kinetic plus thermal energy to gravitational energy) of the initial cloud. Broadly speaking, the effects of these properties are minor. The power spectrum does not significantly affect the clustering statistics of the resulting stars (Schmeja & Klessen 2006), as measured, for example, through the ‘Q’ parameter of Cartwright & Whitworth (2004). In the case of one-off turbulent stirring, the power spectrum also has no effect on the resulting IMF (Bate 2009*c*). If turbulent forcing is sustained, Klessen (2001) found that low-mass star formation is suppressed (i.e., the IMF is flattened) when the turbulent driving is driven on small scales (i.e., comparable with the Jeans length). As noted above, the turbulent Mach number has little effect on the resulting IMF (Bonnell *et al.* 2006) and also does not affect the clustering statistics (Schmeja & Klessen 2006).

The gravitational boundedness of the simulation does, however, affect the degree to which the cluster merger goes to completion (contrast the left- and right-hand portions of figure 2) and has a striking influence on the *star-formation efficiency* (fraction of cloud turning into stars per free-fall time; Clark & Bonnell 2004; Clark *et al.* 2008; see §5 *c* (ii)). The effect of boundedness on the IMF is not clearly established (Clark *et al.* 2008; Maschberger *et al.* 2009).

#### 4. A new generation of simulations: adding extra physics

The simulations described above have several obvious deficiencies. The omission of magnetic fields and the crude treatment of the (barotropic) equation of state encourages profuse fragmentation of dense gas, thus overproducing low-mass stars and overpredicting the importance of dynamical interactions. This is particularly acute in the best-resolved simulations (Bate *et al.* 2003; Bate 2009*a*). It is obviously undesirable that such problems are crudely suppressed by low resolution, as in the large-scale simulations of Bonnell *et al.* (2003, 2008). The recent work of Bate (2009*b*) and Price & Bate (2009; which incorporate radiative transfer and magnetic fields in cluster-formation simulations) represents an important development, whose statistical consequences are still relatively unexplored.

The other drawback of the vanilla calculations is the fact that no feedback from massive stars (either mechanical—winds—or from thermal ionization) is included.

This means that in unmagnetized clouds that are globally bound the star-formation efficiency would go to 100%, thus overpredicting the Galactic star-formation rate by orders of magnitude. (Note that low efficiency can be achieved without feedback for initially unbound clouds: Clark *et al.* 2008; §5 *c*). The omission of feedback also provides no mechanism for limiting individual stellar masses if the simulations were run forward in time to create arbitrarily large-scale clusters. Observationally, however, it is clear that the maximum stellar mass never exceeds 150–200  $M_{\odot}$ , even in very populous clusters (Weidner & Kroupa 2004; Oey & Clarke 2005). Finally, the omission of feedback from massive stars means that the issue of triggered star formation is not addressed.

(a) *Magnetic fields and radiative feedback*

Bate (2009*b*) presented turbulent-fragmentation calculations where the barotropic equation of state was replaced by evolution of the thermal state of the gas and solution of the equations of radiative transfer (in the grey flux-limited diffusion limit; Whitehouse *et al.* 2005). Qualitatively, this allows gas to be radiatively heated by  $p dV$  work liberated deep in the potential of each forming protostar. (Such calculations, however, *underestimate* this effect, since they only include energy liberated outside the sink radius (at a few AU) and omit the effect of thermonuclear and accretion energy released at smaller radius: see Krumholz *et al.* 2007). Even this partial inclusion of radiative feedback changes the simulation outcome quite dramatically at the low-mass end: the modest rise in temperature in the vicinity of each forming low-mass protostar increases the Jeans mass and, hence, suppresses fragmentation locally. This then severely suppresses the formation of brown dwarfs, so that the brown-dwarf-to-star ratio is now  $\sim 1 : 5$ , compared with the ‘vanilla’ (barotropic) calculation that yielded a ratio of  $> 3 : 2$ , in conflict with observations, as discussed above. Note that the gentle thermal feedback from low-mass star formation mainly suppresses new object creation. It neither destroys star-forming cores nor stops accretion onto existing objects.

Price & Bate (2009) performed the first turbulent-fragmentation calculations including a (frozen-in) magnetic field, whose initial amplitude corresponded to a global mass-to-flux ratio of either three or five times that required for collapse. The magnetic field mainly affects the large-scale structure by supporting low-density regions against collapse and thus inhibiting core formation (contrast the panels in figure 8, which show successively less structure as the magnetic field is increased down the page). This reduces the star-formation efficiency so that  $< 10\%$  of the cloud is turned into stars per free-fall time. This star-formation efficiency is in good agreement with observational estimates (e.g., Evans *et al.* 2009), in contrast to field-free calculations (see figure 10).

(b) *Thermal ionization and stellar winds*

OB stars feed back energy into the cluster environment both through the thermal effects of ionizing radiation and via mechanical energy input from energetic winds. In recent years, each of these effects have been incorporated into SPH codes [see Kessel–Deynet & Burkert (2000), Dale *et al.* (2007*b*) and Gritschneder *et al.* (2009*a*) for the case of ionizing radiation and Dale & Bonnell (2008) for winds].

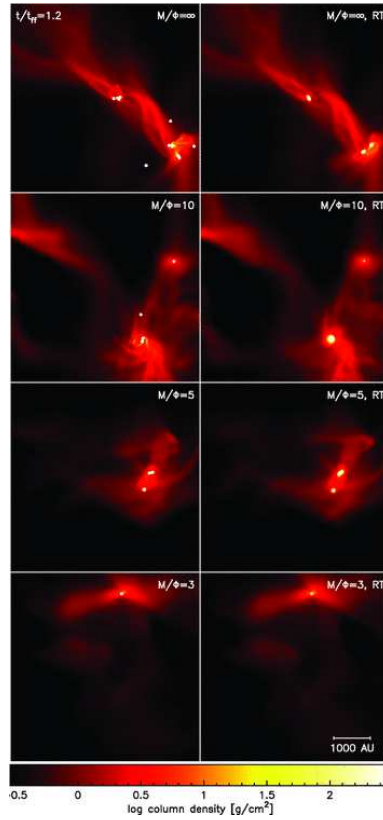


Figure 8. Influence of magnetic fields on cloud evolution, showing suppression of core formation for stronger fields (*lower panels*: Price & Bate 2009).

The impact of ionizing-radiation feedback depends quite sensitively on the location of the ionizing source within the cloud. In the absence of feedback, massive stars tend to be located in cluster cores, at the interception of massive, filamentary accretion flows. The gas distribution seen from such a star is thus highly anisotropic and this significantly affects the impact of its ionizing radiation. Dale *et al.* (2005) found that the dense filaments remain largely neutral and inflowing, while low-density regions are rapidly ionized and drive powerful outflows. This combined inflow–outflow mode means that clouds can remain bound even when they absorb (thermal and kinetic) energy that exceeds their gravitational binding energy. Energy is carried off by a relatively small mass fraction at speeds that comfortably exceed the cluster’s escape velocity. The highly inhomogeneous nature of molecular clouds may thus impede their destruction by ionizing radiation from embedded sources.

Dale *et al.* (2007a) instead examined the case where the ionizing source was located *outside* a molecular cloud. This simulation was globally unbound and so in the control simulation (no ionizing source) the star-formation efficiency was, in any case, low, with much of the cloud simply streaming away from a central star-forming core. When a source of ionizing radiation is introduced, it reverses this outflow on the side of the cloud facing the source and returns the material

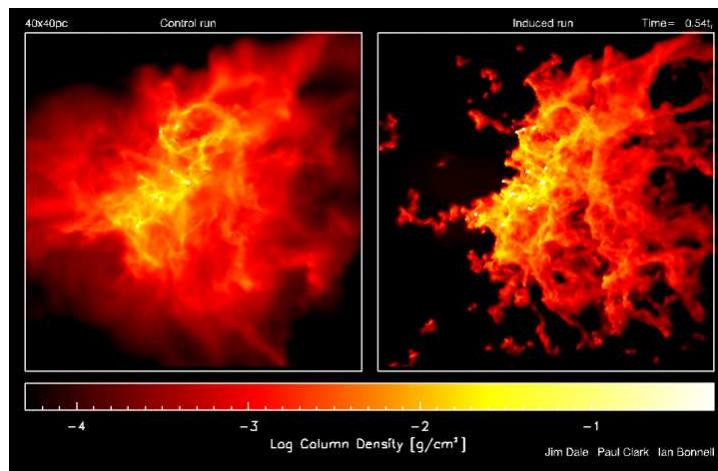


Figure 9. Comparison of cloud structure in the presence of an ionizing source (located to the left of the cloud in the right-hand panel) with a control simulation (*left*). (Dale *et al.* 2007*a.*)

to the dense cloud core, thus boosting the number of stars formed. This is an example of triggered star formation, although the result of net positive feedback *may* be specific to the situation modelled of an initially unbound cloud. Rather disappointingly, no observational properties were found that could distinguish the extra stars that formed as a result of ionization triggering from the stars that formed in the control simulation: both populations were formed in the dense cluster core and with kinematics dominated by the residual turbulent motions in the gas.

Dale & Bonnell (2008) recently included stellar winds in turbulent-fragmentation calculations, switching on winds (either isotropic or collimated) with a mass-dependent mechanical luminosity when stars exceed  $10 M_{\odot}$ . The winds mainly affect the accretion rate onto the wind sources themselves and have little effect on either mass acquisition by lower-mass stars or on the global disruption of the cloud (it is currently unclear whether or not winds play an important role in limiting the maximum stellar mass to its observed value of  $150 - 200 M_{\odot}$ ). The failure of winds to achieve complete disruption of the parent cloud (which might be expected given their high mechanical luminosities) can be traced, as in the case of photoionization discussed above, to the highly inhomogeneous conditions in the cloud. The winds effect efficient energy transfer to the surrounding medium only in the case of low-density regions: these develop powerful outflows of entrained material but do not disrupt the inflow in adjacent dense regions. Although the present pilot simulations are far from being a comprehensive parameter study, these early results perhaps indicate a generic problem, i.e., that (in the case of gravitationally bound clouds with no magnetic field) the initial collapse may be so rapid that it is hard for feedback to reverse the dense anisotropic accretion flows that result.

Finally, we note that the inhomogeneity and complex velocity fields in the simulations mean that the effects of feedback are less visible than in smooth, static media. Although control simulations show that clouds are indeed sculpted by both

winds and photoionization, these do not generally produce the spherical bubble features with which such feedback is conventionally associated.

## 5. Conclusions

### (a) *Observable properties of young star clusters predicted by simulations*

There are generic similarities running through all simulations described above, which make clear predictions about the observational properties of star clusters at an age of  $\sim 0.5$  Myr. The assembly of clusters through scale-free hierarchical merging imparts the resulting clustering with a fractal character, in the sense that the structures have no preferred mass scale and the pattern of nested substructures looks similar at all scales. These clusters are generally mass segregated, except if they are observed shortly after a cluster merger event. The time between such events is, however, longer than the internal mass-segregation timescale, so that mass segregation is the predicted observational norm. The clusters are typically elliptical, their relatively mild flattening (typical axis ratio  $< 2 : 1$ ) being a trade-off between extension in the plane of the most recent merger and ongoing sphericalization by relaxation effects.

### (b) *Implications of cluster-formation simulations for galactic-scale star formation*

#### (i) *The IMF in the field versus clusters*

Most of the clusters formed in these simulations are not long-lived and are expected to contribute to the galactic-field population. The largest clusters are  $\sim 1000 M_{\odot}$  in mass and thus, depending on the subsequent history of gas removal from such objects, they might later be identified observationally as open clusters. Thus, simulations can start to shed light on the formation of both the ‘field’ and ‘cluster’ population in the Galaxy.

In the bottom-up scenario outlined here, essentially all stars are in clusters at some point. Since it is the most populous clusters that are most likely to survive, the ultimate destiny of a particular star as a field or cluster member is largely determined by how many mergers it undergoes, which depends at least partly on the the degree of gravitational boundedness of the parent cloud locally.

Since ‘cluster’ and ‘field’ stars follow similar early evolutionary histories, one does not expect major differences between ‘field’ and ‘cluster’ stars. For example, the closest dynamical interactions (which may determine the formation of binary systems and the possible destruction of protoplanetary discs) often occur in the early formation stages when essentially *all* stars (regardless of their ultimate designation as ‘field’ or ‘cluster’ objects) are in small- $N$  groupings. The lower end of the IMF (as measured by the ratio of stars to brown dwarfs, for example) is thus expected to be similar in rich clusters and what will ultimately become the field. In broad terms, successive cluster mergers do not greatly affect the lowest-mass stars, since these tend not to undergo significant accretion in cluster cores.

The upper end of the IMF *does*, however, depend on the history of successive cluster mergers, since mergers furnish the opportunity for further accretional growth by the most massive stars. Two observational consequences of this scenario are therefore (i) that the slope of the IMF is somewhat flatter in populous clusters



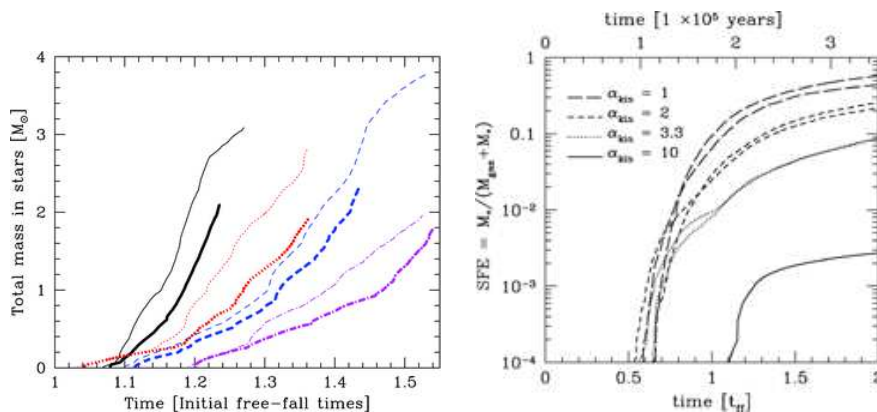


Figure 10. Effect of magnetic-field strength (increasing left to right in the left-hand panel; Price & Bate 2009) and initial ratio of kinetic to gravitational energy (increasing left to right in the right-hand panel; Clark *et al.* 2008) on star-formation efficiency.

than in the total population and (ii) that the IMF in a cluster is truncated at the upper end at a value that depends on cluster richness. Weidner & Kroupa (2005; see also Pflamm–Altenburg *et al.* 2009) have set out a number of potential observational consequences of a scenario in which the integrated galactic IMF is, in fact, steeper than the IMF in individual clusters and may vary with galactic properties [see Hoversten & Glazebrook (2008) for possible observational corroboration of this effect]. The simulations support such a distinction, but in the cases studied so far the difference is rather modest (see figure 5).

Finally, it should be stressed that the above is derived from simulations that omit stellar feedback. Pilot studies involving both ionizing radiation and feedback from stellar winds suggest that the latter may be important in limiting individual stellar masses at the high-mass end and may thus introduce an additional truncation to the stellar IMF that is independent of cluster environment.

#### (ii) *The efficiency of star formation*

The fraction of a cloud that is incorporated in stars per free-fall time is an important quantity since it controls the relationship between the total molecular gas in the Galaxy and the Galactic star-formation rate. Current observational estimates of these quantities imply a star-formation efficiency of  $< 10\%$  (Evans *et al.* 2009). It is found that, in the absence of magnetic fields, simulations starting from gravitationally bound initial conditions form stars much more rapidly than this. In fact, pilot simulations (Dale *et al.* 2005; Dale & Bonnell 2008) suggest that, in this case, the collapse is so rapid that by the stage that feedback from massive stars (photoionization or winds) switches on, it can be hard to disrupt the dense accretion flows and quench the star-formation rate significantly.

Instead, it would seem that low star-formation efficiencies can be achieved either in simulations that start from globally unbound clouds (Clark & Bonnell 2004; Clark *et al.* 2008) or where clouds are threaded by (moderately supercritical) magnetic fields (Price & Bate 2009): see figure 10. Either of these conditions helps to stop runaway collapse in the early stages of cloud evolution and thus may make it easier

for stellar feedback to quench star formation at a later stage. This is, however, speculation: currently, simulations have just reached the stage where they have started to implement these effects separately. Further investigation is required to understand how these processes interact in the formation of stars and clusters from molecular clouds.

## References

- Allison, R., Goodwin, S., Parker, R., de Grijs, R., Portegies Zwart, S. & Kouwenhoven, T. 2009 Dynamical mass segregation on a very short timescale. *Astrophys. J.*, **700**, L99–L103.
- Andersen, M., Neyer, M., Greissl, J. & Aversa, A. 2008 Evidence for a turnover in the initial mass function of low-mass stars and substellar objects: analysis from an ensemble of young clusters. *Astrophys. J.* **683**, L183–L186.
- Bate, M. 1998 Collapse of a molecular cloud core to stellar densities: the first three-dimensional calculations. *Astrophys. J.*, **508**, L95–L98.
- Bate, M. 2009a Stellar, brown dwarf and multiple star properties from hydrodynamical simulations of star cluster formation. *Mon. Not. R. Astron. Soc.*, **392**, 590–616.
- Bate, M. 2009b The importance of radiative feedback for the stellar initial mass function. *Mon. Not. R. Astron. Soc.*, **392**, 1363–1380.
- Bate, M. 2009c The dependence of star formation on initial conditions and molecular cloud structure. *Mon. Not. R. Astron. Soc.*, **397**, 232–248.
- Bate, M. & Bonnell, I. 2005 The origin of the initial mass function and its dependence on the mean Jeans mass in molecular clouds. *Mon. Not. R. Astron. Soc.*, **356**, 1201–1221.
- Bate, M., Bonnell, I. & Price, N. 1995 Modelling accretion in protobinary systems. *Mon. Not. R. Astron. Soc.*, **277**, 362–376.
- Bate, M., Bonnell, I. & Bromm, V. 2002 The formation mechanism of brown dwarfs. *Mon. Not. R. Astron. Soc.*, **332**, L65–L68.
- Bate, M., Bonnell, I. & Bromm, V. 2003 The formation of a star cluster: predicting the properties of stars and brown dwarfs. *Mon. Not. R. Astron. Soc.*, **339**, 577–599.
- Bondi, H. & Hoyle, F. 1944 On the mechanism of accretion by stars. *Mon. Not. R. Astron. Soc.*, **104**, 273–282.
- Boily, C. & Kroupa, P. 2003 The impact of mass loss on star cluster formation. II. Numerical  $N$ -body integration and further applications. *Mon. Not. R. Astron. Soc.*, **338**, 673–686.
- Bonnell, I., Clarke, C., Bate, M. & Pringle, J. 2001 Accretion in stellar clusters and the initial mass function. *Mon. Not. R. Astron. Soc.*, **324**, 573–579.
- Bonnell, I., Bate, M. & Vine, S. 2003 The hierarchical formation of a stellar cluster. *Mon. Not. R. Astron. Soc.*, **346**, L46–L50.
- Bonnell, I., Vine, S. & Bate, M. 2004 Massive star formation: nurture, not nature. *Mon. Not. R. Astron. Soc.*, **349**, 735–741.
- Bonnell, I., Clarke, C. & Bate, M. 2006 The Jeans mass and the origin of the knee in the IMF. *Mon. Not. R. Astron. Soc.*, **368**, 1296–1300.
- Bonnell, I., Clark, P. & Bate, M. 2008 Gravitational fragmentation and the formation of brown dwarfs in stellar clusters. *Mon. Not. R. Astron. Soc.*, **389**, 1556–1562.
- Cartwright, A. & Whitworth, A. 2004 The statistical analysis of star clusters. *Mon. Not. R. Astron. Soc.*, **348**, 589–598.
- Chabrier, G. 2003 Galactic stellar and substellar initial mass function. *Publ. Astron. Soc. Pac.*, **115**, 763–795.

- Chapman, S., Pongracic, H., Disney, M., Nelson, A., Turner, J. & Whitworth, A. 1992 The formation of binary and multiple star systems. *Nature*, **359**, 207–210.
- Clark, P. & Bonnell, I. 2004 Star formation in transient molecular clouds. *Mon. Not. R. Astron. Soc.*, **347**, L36–L40.
- Clark, P., Bonnell, I. & Klessen, R. 2008 The star formation efficiency and its relation to variations in the initial mass function. *Mon. Not. R. Astron. Soc.*, **386**, 3–10.
- Clarke, C. 1999 The fragmentation of cold slabs: application to the formation of clusters. *Mon. Not. R. Astron. Soc.*, **307**, 328–336.
- Clarke, C. & Bromm, V. 2003 The characteristic stellar mass as a function of redshift. *Mon. Not. R. Astron. Soc.*, **343**, 1224–1230.
- Dale, J. & Bonnell, I. 2008 The effect of stellar winds on the formation of a protocluster. *Mon. Not. R. Astron. Soc.*, **391**, 2–13.
- Dale, J., Bonnell, I., Clarke, C. & Bate, M. 2005 Photoionizing feedback in star cluster formation. *Mon. Not. R. Astron. Soc.*, **358**, 291–304.
- Dale, J., Clark, P. & Bonnell, I. 2007a Ionization-induced star formation. II. External irradiation of a turbulent molecular cloud. *Mon. Not. R. Astron. Soc.*, **377**, 535–544.
- Dale, J., Ercolano, B. & Clarke, C. 2007b A new algorithm for modeling photoionizing radiation in smoothed particle hydrodynamics. *Mon. Not. R. Astron. Soc.*, **382**, 1759–1767.
- de Grijs, R. 2010 A revolution in star cluster research: setting the scene. *Phil. Trans. R. Soc. A*, this volume.
- Delgado–Donate, E., Clarke, C. & Bate, M. 2003 Accretion and dynamical interactions in small- $N$  star forming clusters:  $N = 5$ . *Mon. Not. R. Astron. Soc.*, **342**, 926–938.
- Delgado–Donate, E., Clarke, C. & Bate, M. 2004a The dependence of the substellar IMF on the initial conditions for star formation. *Mon. Not. R. Astron. Soc.*, **347**, 759–770.
- Delgado–Donate, E., Clarke, C., Bate, M. & Hodgkin, S. 2004b On the properties of young multiple stars. *Mon. Not. R. Astron. Soc.*, **351**, 617–629.
- Elmegreen, B. & Elmegreen, D. 1978 Star formation in shock-compressed layers. *Astrophys. J.*, **220**, 1051–1062.
- Evans, N., *et al.* 2009. The Spitzer C2D legacy results: star-formation rates and efficiencies; evolution and lifetimes. *Astrophys. J. Suppl. Ser.*, **181**, 321–350.
- Geyer, M. & Burkert, A. 2001 The effect of gas loss on the formation of bound stellar clusters. *Mon. Not. R. Astron. Soc.*, **323**, 988–994.
- Goodwin, S. P. 2010 Binaries in star clusters and the origin of the field stellar population. *Phil. Trans. R. Soc. A*, this volume.
- Goodwin, S. & Bastian, N. 2006 Gas expulsion and the destruction of massive young clusters. *Mon. Not. R. Astron. Soc.*, **373**, 752–758.
- Goodwin, S., Whitworth, A. & Ward–Thompson, D. 2004a Simulating star formation in molecular cloud cores. I. The influence of low levels of turbulence on fragmentation and multiplicity. *Astron. Astrophys.*, **414**, 633–650.
- Goodwin, S., Whitworth, A. & Ward–Thompson, D., 2004b). Simulating star formation in molecular cores. II. The effects of different levels of turbulence. *Astron. Astrophys.*, **423**, 169–182.
- Goodwin, S., Whitworth, A. & Ward–Thompson, D. 2006 Star formation in molecular cores. III. The effect of the turbulent power spectrum. *Astron. Astrophys.*, **452**, 487–492.
- Gritschneider, M., Naab, T., Burkert, A., Walch, S., Heitsch, F. & Wetzstein, M. 2009 iVINE: Ionization in the parallel TREE/SPH code VINE: first results on the observed age spread around O-stars. *Mon. Not. R. Astron. Soc.*, **393**, 21–31.
- Gritschneider, M., Naab, T., Walch, S., Burkert, A. & Heitsch, F. 2009 Driving turbulence and triggering star formation by ionizing radiation. *Astrophys. J.*, **694**, L26–L30.

- Heyer, M. & Brunt, C. 2004 The universality of turbulence in Galactic molecular clouds. *Astrophys. J.*, **615**, L45–L48.
- Heyer, M., Carpenter, J. & Snell, R. 2001 The equilibrium state of molecular regions in the outer Galaxy. *Astrophys. J.*, **551**, 852–866.
- Hoversten, E. & Glazebrook, K. 2008 Evidence for a nonuniversal stellar initial mass function from the integrated properties of SDSS galaxies. *Astrophys. J.*, **675**, 163–187.
- Kessel–Deynet, O. & Burkert, A. 2000 Ionizing radiation in smoothed particle hydrodynamics. *Mon. Not. R. Astron. Soc.*, **315**, 713–721.
- Kitsionas, S., Federrath, C., Klessen, R., Schmidt, W., Price, D., Dursi, J., Gritschneider, M., Walch, S., Piontek, R., Kim, J., Jappsen, A.-K., Cieleciag, P. & Mac Low, M.-M. 2008 Algorithmic comparisons of decaying, isothermal, compressible turbulence. I. Low-resolution simulations with fixed grids. *Astron. Astrophys.*, in press (arXiv:0810.4599).
- Klessen, R. & Burkert, A. 2000 The Formation of stellar clusters: Gaussian cloud conditions. I. *Astrophys. J. Suppl. Ser.*, **128**, 287–319.
- Klessen, R. & Burkert, A. 2001 The formation of stellar clusters: Gaussian cloud conditions. II. *Astrophys. J.*, **549**, 386–401.
- Klessen, R., Burkert, A. & Bate, M. 1998 Fragmentation of molecular clouds: the initial phase of a stellar cluster. *Astrophys. J.*, **501**, L205–L208.
- Kritsuk, A., Norman, M., Padoan, P. & Wagner, R. 2007 The statistics of supersonic isothermal turbulence. *Astrophys. J.*, **665**, 416–431.
- Kroupa, P. 2002 The initial mass function of stars: evidence for uniformity in variable systems. *Science*, **295**, 82–91.
- Kroupa, P. & Weidner, C. 2003 Galactic-field initial mass functions of massive stars. *Astrophys. J.*, **598**, 1076–1078.
- Kroupa, P., Tout, C. & Gilmore, G. 1993 The distribution of low-mass stars in the Galactic disc. *Mon. Not. R. Astron. Soc.*, **262**, 545–587.
- Krumholz, M., Klein, R. & McKee, C. 2007 Radiation-hydrodynamic simulations of collapse and fragmentation in massive protostellar cores. *Astrophys. J.*, **665**, 478–491.
- Lada, C. J. 2010 The physics and modes of star cluster formation: observations. *Phil. Trans. R. Soc. A*, this volume.
- Lada, C., Munech, A., Rathbone, J., Alves, J. & Lombardi, M. 2008 The nature of the dense core population in the Pipe Nebula: thermal cores under pressure. *Astrophys. J.*, **672**, 410–422.
- Larson, R. 1981 Turbulence and star formation in molecular clouds. *Mon. Not. R. Astron. Soc.*, **194**, 809–826.
- Larson, R. 2005 Thermal physics, cloud geometry and the stellar initial mass function. *Mon. Not. R. Astron. Soc.*, **359**, 211–222.
- Lemaster, N. & Stone, J. 2008 Density probability distribution functions in supersonic hydrodynamic and MHD turbulence. *Astrophys. J.*, **682**, L97–L100.
- Lubow, S. & Pringle, J. 1993 The gravitational stability of a compressed slab of gas. *Mon. Not. R. Astron. Soc.*, **263**, 701–706.
- Masunaga, H. & Inutsuka, S. 2000 A radiation hydrodynamic model for protostellar collapse. II. The second collapse and the birth of a protostar. *Astrophys. J.*, **531**, 350–365.
- Maschberger, T., Clarke, C. & Bonnell, I. 2009 The properties of star clusters in turbulent fragmentation calculations. in prep.
- Motte, F., André, P. & Neri, R. 1998 The initial conditions of star formation in the rho Ophiuchi main cloud: wide-field millimeter continuum mapping. *Astron. Astrophys.*, **336**, 150–172.
- Muench, A., Lada, E., Lada, C. & Alves, J. 2002 The luminosity and mass function of the Trapezium cluster: from B stars to the deuterium-burning limit. *Astrophys. J.*, **573**, 366–393.

- Oey, S. & Clarke, C. 2005 Statistical confirmation of a stellar upper mass limit. *Astrophys. J.*, **620**, L43–L46.
- Offner, S., Hansen, C. & Krumholz, M. 2009 Stellar kinematics of young clusters in turbulent hydrodynamic simulations. *Astrophys. J.*, **704**, L124–L128.
- Padoan, P., Nordlund, A. & Jones, B. 1997 The universality of the stellar initial mass function. *Mon. Not. R. Astron. Soc.*, **288**, 145–152.
- Pflamm-Altenburg, J., Weidner, C. & Kroupa, P. 2009 *Mon. Not. R. Astron. Soc.*, **395**, 394–400.
- Price, D. & Bate, M. 2009 Inefficient star formation: the combined effects of magnetic fields and radiative feedback. *Mon. Not. R. Astron. Soc.*, **398**, 33–46.
- Reipurth, B. & Clarke, C. 2001 The formation of brown dwarfs as ejected stellar embryos. *Astron. J.*, **122**, 432–439.
- Salpeter, E. 1955 The luminosity function and stellar evolution. *Astrophys. J.*, **121**, 161–167.
- Schmeja, S. & Klessen, R. 2004 Protostellar mass accretion rates from gravoturbulent fragmentation. *Astron. Astrophys.*, **419**, 405–417.
- Schmeja, S. & Klessen, R. 2006 Evolving structures of star-forming clusters. *Astron. Astrophys.*, **449**, 151–159.
- Smith, R., Clark, P. & Bonnell, I. 2008 The structure of molecular clouds and the universality of the clump mass function. *Mon. Not. R. Astron. Soc.*, **391**, 1091–1099.
- Weidner, C. & Kroupa, P. 2004 Evidence for a fundamental stellar upper mass limit from clustered star formation. *Mon. Not. R. Astron. Soc.*, **348**, 187–191.
- Weidner, C. & Kroupa, P. 2005 The variation of integrated star initial mass functions among galaxies. *Astrophys. J.*, **625**, 754–762.
- Weidner, C. & Kroupa, P. 2006 The maximum stellar mass, star-cluster formation and composite stellar populations. *Mon. Not. R. Astron. Soc.*, **365**, 1333–1347.
- Whitehouse, S., Bate, M. & Monaghan, J. 2005 A faster algorithm for smoothed particle hydrodynamics with radiative transfer in the flux-limited diffusion approximation. *Mon. Not. R. Astron. Soc.*, **364**, 1367–1377.
- Whitworth, A., Boffin, H. & Francis, N. 1998 Gas cooling by dust during dynamical fragmentation. *Mon. Not. R. Astron. Soc.*, **299**, 554–561.
- Zinnecker, H. 1982 Prediction of the protostellar mass spectrum in the Orion near-infrared cluster. *NY Acad. Sci. Ann.*, **395**, 226–235, New York: New York Acad. Sci.